REPRODUCTION
RESEARCH

Ultrastructure of spermatogenesis in Spix's yellow-toothed cavy (*Galea spixii*)

P R S Santos, M F Oliveira[1], M A M Arroyo, A R Silva[1], R E G Rici, M A Miglino and A C Assis Neto

Department of Surgery, School of Veterinary Medicine and Animal Science, University of São Paulo, Av. Prof. Dr Orlando Marques de Paiva 87, 05508 270 São Paulo, Brazil and [1]Department of Animal Science, Federal Rural University of the Semi-arid Northeastern Region (UFERSA), Av. Francisco Mota 52, 59625 900 Mossoró, Brazil

Correspondence should be addressed to A C Assis Neto; Email: antonioassis@usp.br

Abstract

This was a pioneer study of the spermatogenic process from the onset of puberty in Spix's yellow-toothed cavies (SYC, *Galea spixii*) bred in captivity. The study aimed to characterize fine structure of spermatogenesis. Twelve testes from pubertal and post-pubertal SYC males were studied using transmission electron microscopy. Spermatogenesis can be divided into three phases: proliferation, meiosis, and spermiogenesis. In proliferation phase, three types of spermatogonia were identified and characterized as A_{dark}, A_{pale}, and B. In the second phase, spermatocytes (2n) undergo meiotic divisions that generate spermatids (n); the process begins in spermatocytes in the preleptotene stage when they increase their nuclear size, differentiating into spermatocytes in the leptotene stage when cell division is initiated. In addition, we found chromatin condensation, and formation of a structure composed of proteins that formed a central shaft and two lateral bars associated with pairing of homologous chromosomes. During spermiogenesis, the following main events occurred: condensation of nuclear chromatin, formation of acrosome with perforatorium, elimination of residual cytoplasm, and development of the flagellum. The sperm head is different from that of other rodents. The endoplasmic reticulum and the Golgi complex are the two main organelles demonstrated during this process. These organelles collaborate through synthesis of proteins and hormones for the development of germ cells during spermatogenesis in SYC.

Reproduction (2014) **147** 13–19

Introduction

Spix's yellow-toothed cavy (SYC, *Galea spixii*) is found in the regions of northeastern Brazil (Eisenberg & Rerdford 1999). It is an herbivorous species with gray hair and a ring of white hairs around the eyes. When mature, cavies are 22.5–23.5 cm long, weigh between 375 and 405 g, and breed throughout the year, with a gestation period of ∼48 days (Oliveira *et al*. 2008).

Although consumed as an alternative source of animal protein, Red List (IUCN 2013) has declared SYC as an endangered species. Nonetheless, the knowledge of reproductive biology and physiology is important for conservation and species management in captivity; such knowledge also aids efforts to ensure the propagation of endangered species (Busso *et al*. 2005, Wildt 2005).

However, due to risk of extinction of species and use of the same as an alternative source of animal protein, the search for information of captive breeding of these rodents has increased (Carvalho *et al*. 2003). Moreover, this serves as a model for biological discovery of therapies and prevention strategies for various diseases in humans (Domingues & Caldas-Bussiere 2007). For wild rodents, the cavy served as a model in studies of immunology (Von Ubisch & Amaral 1935) and chromatography (Cavalcanti *et al*. 1959) and in cases of leptospirosis (Castro *et al*. 1961). Aside from the work cited earlier, studies related to general biology of the species still lack. On this point, information of general biology, enhancement, preservation, and maintenance in captivity of any kind requires a basic knowledge of reproductive physiology.

Studies related to male SYC have described the establishment of puberty, the seminiferous epithelium cycle, and genital organs (Santos *et al*. 2011, 2012*a*, 2012*b*). For male animals, the study of spermatogenesis is particularly relevant to reproduction of the species, and in this regard, the ultrastructure view can promote morphological basic information necessary for reproduction biotechnologies. Thus, this study aimed to describe the process of germ cell differentiation in SYC ultrastructurally in order to determine the steps of spermatogenesis.

Materials and methods

Animals, tissue collection, and processing

Twelve pubertal and post-pubertal male specimens of *G. spixii* were studied. The animals were collected in northeastern

ISSN 1470–1626 (paper) 1741–7899 (online)
DOI: 10.1530/REP-13-0452
Online version via www.reproduction-online.org

Brazil (37°20′39″W, 6°12′43″S), in Mossoró City, Rio Grande do Norte, and were held in the histology laboratory at the University of São Paulo (FMVZ/USP).

The Ethics Committee for the Use of Animals at the University of São Paulo (FMVZ/USP) authorized all experimental procedures (protocol: 2486/2011), and the capture and captivity of the cavies were authorized by the Brazilian Institution responsible for wild animal care (Instituto Brasileiro do Meio Ambiente, IBAMA, protocol: 2028236/2008).

The testes of animals (45–150 days old) were collected by orchiectomy and weighed. During the procedure, the older animals were anesthetized with 0.025 mg/ml atropine sulfate (s.c.) and 0.2 ml/kg Zoletil (i.m.). Subsequently, the testes of each animal were fixed by immersion in a solution of 2.5% glutaraldehyde for 24 h.

The tissues were post-fixed in 1% osmium tetroxide solution for 2 h at 4 °C followed by immersion in 5% aqueous uranyl acetate for 24–48 h. Then, the tissues were dehydrated in an increasing series of alcohol, treated with propylene oxide, and infiltrated with a 1:1 mixture of pure resin and propylene oxide, and after embedding in Spurr resin, they were kept in an oven at 60 °C for 3–5 days until complete polymerization. Thick sections of 1–3 μm were obtained with a diamond razor in an ultramicrotome (Leica EM Ultracut, Vienna, Austria) and stained with toluidine blue solution for light microscope analysis. Ultrathin sections (60 nm) were collected in mesh grids, contrasted with uranyl acetate and lead citrate solutions (Watanabe & Yamada 1983), and examined with a Morgagni 268D (FEI, Hillsboro, OR, USA) transmission electron microscopy (TEM) at the Faculty of Medicine Veterinary and Animal Science, University of Sao Paulo (FMVZ/USP).

Results

Testis

The testicular parenchyma consists of germ cells, Sertoli cells, Leydig cells, myoid cells, and vessels. During puberty, the seminiferous tubules with lumen and germ cells at different stages of division were noted and showed different stages of the seminiferous epithelium cycle (Fig. 1A). The myoid cells showed a cytoplasm with parallel filaments and a fusiform nucleus, with chromatin distributed throughout its length (Fig. 1B).

Spermatogonia

At the ultrastructural level, only three types of spermatogonia can be identified accurately in SYC: spermatogonia type A 'dark', spermatogonia type A 'pale', and spermatogonia type B (Fig. 2). Spermatogonia type A 'dark' were elliptical in shape and adhered to the basal lamina, which had irregular projections and depressions. Sertoli cells were located close to the basal area of the germinal epithelium (Fig. 2A). The spermatogonia featured an oval center containing a fine, granular chromatin and 'groups' of condensed chromatin. The single nucleolus was large, granular, and irregular, usually centrally located. The cytoplasm had small mitochondria with few organelles and some extensions of the endoplasmic reticulum (smooth (sER) and rough (rER)).

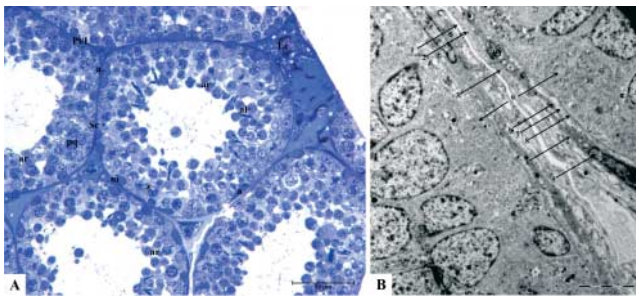

Figure 1 Testis of Spix's yellow-toothed cavy (SYC, *Galea spixii*) featured in the pubertal sexual phase. (A) Testicular parenchyma composed of seminiferous tubules and interstitium. Note the different stages of seminiferous epithelium cycle with germ cells at different stages of differentiation (a, spermatogonia; Pl/L, primary spermatocytes in preleptotene/leptotene; pq, spermatocytes at pachytene; z, spermatocytes at zygotene; ar, round spermatids; al, elongated spermatids; Sc, Sertoli cells; Lc, Leydig cell; m, myoid cell; spz, spermatozoa), semi-thin section, toluidine blue, scale bars: 50 μm. (B) The base of two adjoining seminiferous tubules showing the boundary tissue (1, lymphatic space; 2, endothelium bounding the lymphatic space; 3, collagen layer; 4, basement membrane; 5, myoid cell; 6, basement membrane; 7, collagen layer; 8, basement membrane; 9, cells constituting the seminiferous tubule), transmission electron microscopy; scale bars: 5 μm.

Spermatogonia type A 'pale' had an elongated shape and less adhesion to the basal lamina when compared with spermatogonia type A 'dark', which were close to the Sertoli cells and the basal area of the seminiferous tubules (Fig. 2B). The pale spermatogonia had an oval nucleus containing homogeneous granular chromatin. Rarely, a large granular nucleoli was seen (Fig. 2B). The cytoplasm contained larger mitochondria, extensions of the ER (rER and sER), Golgi apparatus, and centrioles.

Spermatogonia type B had the least adhesion of cells to the basal lamina. They were usually surrounded by Sertoli cells and had a round nucleus containing homogeneous chromatin with condensed chromatin points near the nuclear envelope (Fig. 2C). The nucleolus was large, granular, and centrally located, and the cytoplasm was similar to other spermatogonia.

Spermatocytes

Spermatocytes developed from the differentiation of spermatogonia during the first meiotic division. Chromatin condensation occurs at this stage, and the formation of the synaptonemal complex, a structure composed of proteins that form a central shaft and two lateral bars associated with chromosome pairing of homologous chromosomes. The preleptotene spermatocyte had a circular shape with a circular core containing homogeneous chromatin. The cytoplasm was accompanied by a few small organelles (Fig. 3A).

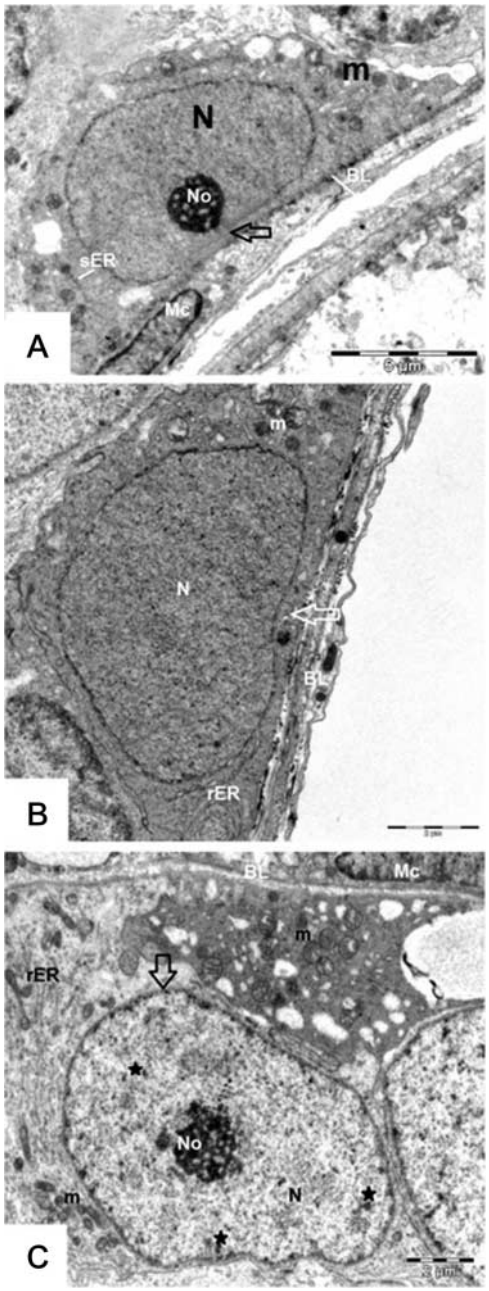

Figure 2 Spermatogenic lineage cells, pre-meiotic cells, Spix's yellow-toothed cavy (SYC, *Galea spixii*). A decrease in the adhesion of basal lamina from type A to type B spermatogonia was observed (arrows). (A) Type A 'dark' (Ad) spermatogonia. (B) Type A 'pale' (Ap) spermatogonia. (C) Type B spermatogonia. Clusters of condensed chromatin and chromatin condensation points were present in the nucleus (star). BL, basal lamina; m, mitochondria; N, nucleus; No, nucleolus; rER, rough endoplasmic reticulum; sER, smooth ER; Mc, myoid cells. Transmission electron microscopy; scale bars: A, 5 µm; B, 2 µm; and C, 2 µm.

The core of the leptotene spermatocyte was larger, demonstrating the beginning of chromatin condensation, which occurred gradually during the transition of zygotene spermatocytes to diakinesis spermatocytes (Fig. 3B). The organization of the nucleolus was apparent even among preleptotene and zygotene spermatocytes (Fig. 3C). The disorganization and break-up of the nucleolus began in pachytene spermatocytes, and the nucleolus lost its morphology and became more fragmented (Fig. 3D).

Diplotene spermatocytes and diakinesis spermatocytes had nucleoli fragments that may have been associated with specific chromosomal regions (Fig. 3E). In diakinesis, there was a reduction in the number of nucleoli fragments. In some areas, it is found associated with a single chromosomal region (Fig. 3F). At this stage, chromosome pairing was observed (Fig. 3F).

Spermatids

Morphological changes, such as the formation of the flagellum and the acrosome, chromatin condensation,

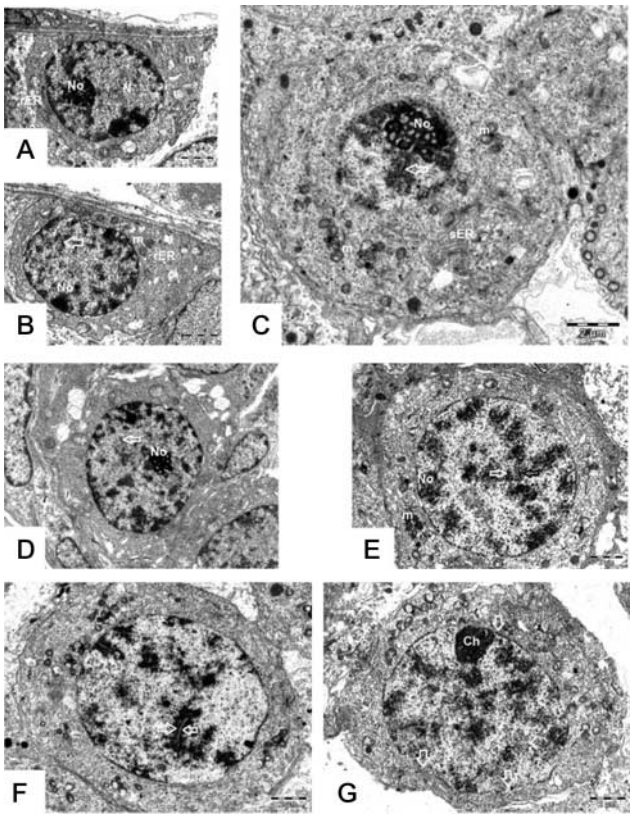

Figure 3 Spermatogenic lineage cells, meiotic cells (meiosis I), Spix's yellow-toothed cavy (SYC, *Galea spixii*). (A) Preleptotene spermatocytes. (B) Leptotene spermatocytes. (C) Zygotene spermatocytes. (D) Pachytene spermatocytes. (E) Diplotene spermatocytes. (F) Spermatocytes in diakinesis. (G) Spermatocytes in metaphase. A disorganization of the nucleolus was noted (nucleolar material scattered) from leptotene to diplotene, with certain parts associated with a single chromosomal region in diakinesis (F), the structural framework among the chromosomes in diakinesis (F), and the nuclear envelope breaks in metaphase (G (arrow)) with centrioles positioned at the opposite pole of the cell (C, centrioles; Ch, chromosomes; m, mitochondrion; rER, rough ER; sER, smooth ER; No, nucleolus). Transmission electron microscopy; scale bars: 2 µm.

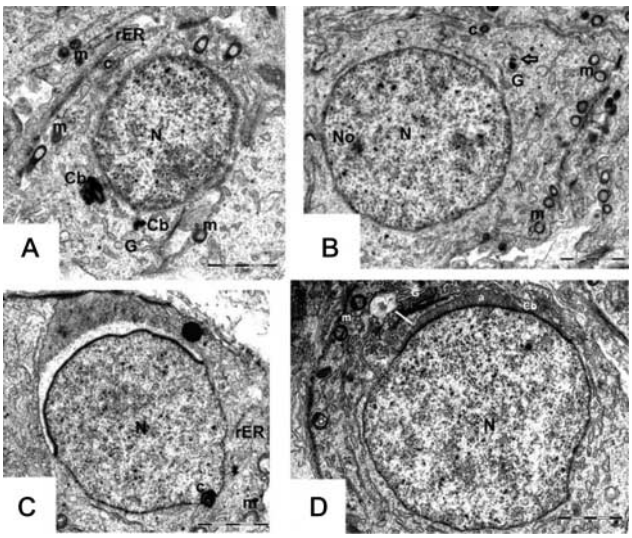

Figure 4 Spermatogenic lineage cells, meiotic cells (meiosis II), Spix's yellow-toothed cavy (SYC, *Galea spixii*). (A) Spermatids Step I: note the low differentiation of spermatids of this type. The cores are spherical and the chromatoid body and the Golgi complex are closely related. The centrioles are seen near the plasma membrane and mitochondria are scattered throughout the cytoplasm. (B) Spermatids Step II: observe the development of the Golgi apparatus and centrioles were displaced to the vicinity of the Golgi complex. (C) Spermatids Step III: note the polar shift of centrioles for formation of the acrosome, facilitating development of the axoneme. (D) Spermatids Step IV: proacrosomal vacuoles are round and compact, joining the nuclear envelope (arrows). Note the close proximity of the chromatoid body to the region of acrosome formation (a, acrosome; C, centrioles; Cb, chromatoid body; G, Golgi apparatus; m, mitochondria; N, nucleus; No, nucleolus; PV, proacrosomal vacuole; rER, rough ER). Transmission electron microscopy; scale bars: 2 μm.

nuclear elongation, and removal of the cytoplasm, occurred during spermatid differentiation. Our results showed that this process is divided into four phases: the Golgi phase, the cap phase, the acrosomal phase, and the maturation phase (Figs 4 and 5).

In Golgi phase, spermatids originated from the second meiotic division. They had a spherical nucleus with condensed chromatin points, and a region of concentrated chromatin was seen near the nuclear envelope. The Golgi complex was developing, increasing in size, and blisters began to fuse to form the proacrosomal vesicles. The centrioles tended to be located close to pole opposite the formation of the axoneme. The distal centriole initiated the formation of the axoneme (Fig. 4A, B and C).

In cap phase, spermatids had a developed Golgi apparatus with highest production of proacrosomal vesicles joining the nuclear envelope to make the cell nucleus concave. Note the formation of the acrosome. The acrosome began to cover the core, surrounding almost the entire surface (Figs 4D and 5A).

In acrosomal phase, the acrosome condensed in a strong, dense, and granular arrangement. It can be seen at the beginning of the disorganization of the nucleolus. The acrosome covered much of the nuclear surface in association with microtubules in the distal region, and the nuclear elongation of the spermatid occurred in this phase (Fig. 5B, C and D).

The acrosome covered the entire core and the nucleolus could not be seen in the maturation phase (Fig. 5E, F and G). Spermatids were elongated, and the heads had prominent perforatorium. In this phase, the spermatids become similar to spermatozoa. The mitochondrial sheath was organized in the middle part, and a fibrous sheath formed the main part. There was great change in the cytoplasm when compared with spermatids in the other steps. It was the last phase before the release of sperm into the tubular lumen.

Spermatozoa

The spermatozoa consisted of a head, neck, intermediate part, main part, and an end part. The head with a fusiform shape was covered externally by a plasma membrane on top of the core, with a space separating the outer acrosomal membrane and the equatorial segment connecting to the end portion in the terminal region of the acrosome.

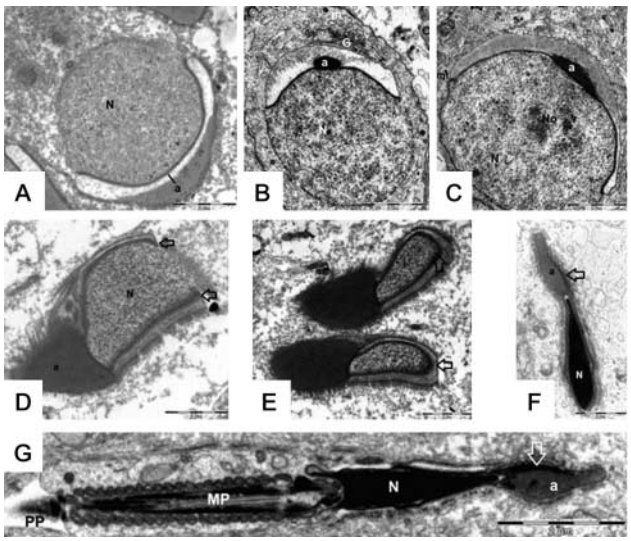

Figure 5 Spermatogenic lineage cells, meiotic cells (meiosis II) continued, Spix's yellow-toothed cavy (SYC, *Galea spixii*). (A) Spermatids Step V: note the intimate association of the acrosome with the nuclear envelope. (B) Spermatids Step VI: condensation and expansion of the acrosome. (C) Spermatids Step VII: migration of the nucleus to the plasma membrane and early nucleolar disorganization. (D) Spermatids Step IX: elongation of the nuclear acrosome within the nucleus (arrow), assuming an arrow shape. (E) Spermatids Step X: the nuclear ring completes its shift to the posterior region of the nucleus (arrow). (F) Spermatids Step XI: head of spermatid has a prominent perforatorium (arrow). (G) Spermatids Step XII: spermatids reach the shape of the sperm, the mitochondrial sheath of the middle piece, and the fibrous sheath (a, acrosome; m, mitochondria; N, nucleus; No, nucleolus; MP, middle piece; arrow, 'perforatorium'; PP, main piece). Transmission electron microscopy; scale bars: 2 μm.

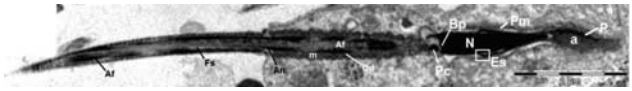

Figure 6 Ultrastructure of spermatozoa, Spix's yellow-toothed cavy (SYC, *Galea spixii*). Longitudinal section of the spermatozoon (a, acrosome; Af, axial filament; An, ring; Bp, basal plate; Es, equatorial segment; Fs, fibrous sheath; m, mitochondria; N, nucleus; Od, outer dense fibers; P, perforatorium; Pc, proximal centriole; Pm, plasma membrane). Transmission electron microscopy; scale bars: 2 μm.

Extending from the inner acrosomal membrane into the middle of the acrosome is the perforatorium. The core was chromatin dense and homogeneous in shape (Fig. 6). The neck was located in the hollow core of the base where the proximal centriole attached to the basal plate and the nuclear membrane. The middle piece was shorter and contained mitochondrial pairs. The diameter decreased in the tail.

The main piece was higher than the intermediate part. A dense fiber extended outward from the fibrous sheath, decreasing and disappearing in the end portion of the main part. The end of the tail, which was difficult to observe, consisted of an axial filament enclosed by plasma membrane (Fig. 6).

Sertoli and Leydig cells

At the pubertal stage, the Sertoli cells remained attached to the basal membrane, where they had cytoplasmic extensions involving the germ cells. The core was large and triangular in shape, with a homogeneous euchromatin nucleoplasm. The nucleolus appeared scattered, occupying part of the nuclear area. The cytoplasm contained subcellular structures such as the ER, Golgi apparatus, mitochondria, and ribosomes (Fig. 7A).

Leydig cells were paired and associated with blood vessels. The Leydig cells show round and oval nuclei. In the cytoplasmic compartment, the Golgi complex, an extensive sER, and few lipids were observed. The Leydig cells filled most of the interstitial space into a smaller intercellular space between the seminiferous tubules (Fig. 7B).

Discussion

Previous studies in SYC have been carried out on sexual and testicular development (Santos *et al*. 2012*a*), frequency and stages of the seminiferous epithelium cycle (Santos *et al*. 2011), and development of male genital organs (Santos *et al*. 2012*b*). This study permitted the description of the spermatogenic process from the onset of puberty in SYC bred in captivity, thus contributing to the knowledge of reproductive biology.

The spermatogenic process of SYC, as well as other mammals, can be divided into three phases: proliferation, meiosis, and spermatogenesis (Clermont 1972). The proliferation phase had three spermatogonia types: Ad (dark), Ap (pale), and B, identified by the nuclear morphology of chromatin condensation and position within the seminiferous epithelium (Smithwick *et al*. 1996). At this phase, there was an increase in the number of mitochondria, and this contributes to the increase in ATP nuclear promoting cell proliferation (Warburg 1966).

The second phase of spermatogenesis, the meiotic phase, is the process wherein spermatocytes (2n) undergo meiotic divisions that generate spermatids (n) (Russell *et al*. 1990). The process begins in spermatocytes in the preleptotene stage when they increase their nuclear size, differentiating into spermatocytes in the leptotene stage when cell division initiates. The nuclear characteristics of spermatocytes were similar to those of rodents and other mammals (Schleirmacher & Schmidt 1973, Solari & Moses 1973).

In the last stage of spermiogenesis, a round spermatid differentiates into a spermatozoon capable of fertilization (Clermont 1972). The spermatid differentiation occurred in four phases: the Golgi phase, the cap phase, the acrosomal phase, and the maturation phase (Gunawardana & Scott 1977, Singwi & Lall 1983, Lin & Jones 1993, Góes & Dolder 2002, Segatelli *et al*. 2002). Chromatoid bodies observed in spermatids have been reported in guinea pigs, other mammals, birds, and reptiles. Moreover, the presence of chromatoid bodies promote the part connection in mature spermatozoa (Sud 1961, Fawcett *et al*. 1970).

During this process, the following events occurred: condensation of the nuclear chromatin, formation of the acrosome, elimination of residual cytoplasm, and development of the flagellum procedure. The process is similar to that of the rodents (Lalli & Clermont 1981).

The spermatozoa is the final process of spermatogenesis, which occurs through the meiotic and mitotic divisions in the seminiferous epithelium of the testis (Eddy 2006). The sperm head of SYC is fusiform shaped, differing from other rodents such as rats, mice, and hamsters (Pesch & Bergmann 2006), which have

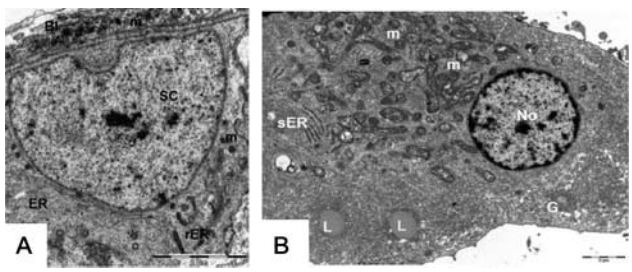

Figure 7 Sertoli and Leydig cells in Spix's yellow-toothed cavy (SYC, *Galea spixii*). (A) There is a triangular nucleus, nucleolus with condensed chromatin, and the presence of many mitochondria in the cytoplasm. Adherence to the basal lamina and a greater cytoplasmic area. (B) Many groups of mitochondria are associated with the ER. Few lipid droplets were seen. BL, basal lamina; m, mitochondria; N nucleus; No, nucleolus; rER, rough endoplasmic reticulum; sER, smooth ER; LC, Leydig cells; L, lipid droplets; v, vesicles. Transmission electron microscopy; scale bars: 2 μm.

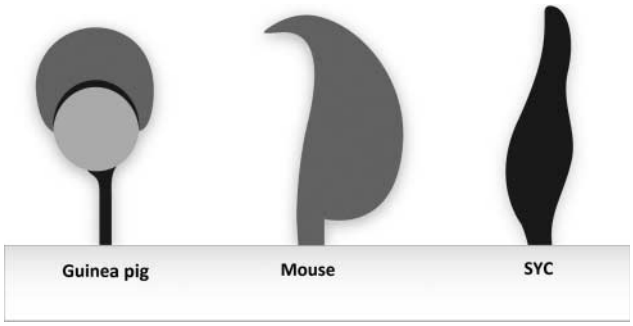

Figure 8 The sperm head of rodents. The spatulate-shaped heads of guinea pig; the falciform-shaped heads of mouse; and the fusiform-shaped heads of Spix's yellow-toothed cavy (SYC, *Galea spixii*). The spermatozoon head size and shape is specific to each species.

falciform-shaped heads, and guinea pig, even if belonging to the same subfamily, has spatulate-shaped head (Fig. 8). The acrosome of *G. spixii* shows a large apical segment similar to chinchilla and ground squirrel (Eddy 2006). This morphology of acrosome used to be associated with the vesicles containing enzymes important for sperm fertilization.

The organization and modification of Sertoli cells during spermatogenesis in SYC were similar to those described in mammals in general (Russell & Griswold 1993). The present results suggested that, based on their structural organization, the Sertoli cells may play a role in regulating spermatogenesis, simultaneously contributing to germ cell maturation. The Sertoli cells underwent modifications such as an extension of the ER and the development of mitochondria with tubular cristae. In this respect, it could be argued that the cellular elements derived from Sertoli cells actively support spermatogenesis (França & Russell 1998).

Along with the Sertoli cells, the myoid cells are responsible for the formation of the basal lamina, being a major component of the membrane of the seminiferous tubules (Maekawa *et al.* 1996). Collagen bundles were observed in the interstitium, and myoid cells as well as other components of the extracellular matrix (fibronectin and laminin) produce these. The myoid cells secrete growth factors (TGFβ, IGF1, and activin-A) that regulate the paracrine function of Sertoli cells and express cytoskeletal markers, which act in the contraction of seminiferous tubules and in the conduct of sperm (Maekawa *et al.* 1996, Skinner 2005).

In SYC, Leydig cells showed a developed sER and were directly related to the production of testosterone (Zirkin *et al.* 1980). The sparse amounts of lipids suggest a steroidogenesis functionality or an active androgen pathway. In marsupials, androgens have low levels until puberty, coinciding with the high levels of lipids in this phase (Williamson *et al.* 1990, Renfree *et al.* 1992).

The mitosis, meiosis, and spermiogenesis were described by TEM and highlighted the first occurrence of spermatogenesis in SYC. The sperm heads were different from those of other rodents. In addition, to allow for a usual spermatogenesis, an interaction between the germ cells and Sertoli cells, Leydig cells, and myoid cells is necessary. These cells demonstrated activity in support of spermatogenesis, and followed that of other mammals (Fawcett *et al.* 1970, Hoffer 1982).

Declaration of interest

The authors declare that they have no conflict of interest with relation to the development and publication of the study.

Funding

This work was supported by FAPESP (São Paulo State Research Foundation) grants 2010/14516-0 and 2012/11217-8.

Acknowledgements

The authors thank members of the University of Sao Paulo (FMVZ), Brazil for technical support. They warmly thank Ms Rose Kastelic for help with the English language.

References

Busso JM, Ponzio MF, Cuneo MF & Ruiz RD 2005 Year-round testicular volume and semen quality evaluations in captive *Chinchilla lanigera*. *Animal Reproduction Science* **90** 127–134. (doi:10.1016/j.anireprosci.2005.02.001)

Carvalho AF, Lima MC, Santos TC, Bonatelli M, Miglino MA, Samoto VY, Oliveira MF, Ambrósio CE, Pereira FTV & Martins JFP 2003 Análise microscópica do ovário de cateto em fase gestacional. *Revista Brasileira Reprodução Animal* **27** 278–279.

Castro AFP, Santa Rosa CA & Troise C 1961 Preás (*Cavia aperea aperea*, Linch) Rodentia – Cavidae – como reservatório de leptospira em São Paulo. *Arquivos do Instituto Biológico* **28** 219–222.

Cavalcanti RC, Almeida GR & Martins GF 1959 Cromatografia sobre papel de aminoácidos das proteínas da musculatura uterina (*Cavia aperea aperea* – Rodentia) em biotério, utilizando ração balanceada. Análise de curvas ponderais. *Anais da Faculdade de Medicina do Recife* **19** 297–301.

Clermont Y 1972 Kinetics of spermatogenesis in mammals: seminiferous epithelium cycle and spermatogonial renewal. *Physiological Reviews* **52** 198–236.

Domingues SFS & Caldas-Bussiere MC 2007 Fisiologia e biotécnicas da reprodução desenvolvidas em fêmeas de primatas neotropicais importantes para a pesquisa biomédica. *Revista Brasileira Reprodução* **30** 57–71.

Eddy EM 2006 Chapter 1 – the spermatozoon. In *Knobil and Neill's Physiology of Reproduction*, pp 3–54. Eds E Knobil& JD Neill. St Louis: Academic Press (http://dx.doi.org/10.1016/B978-012515400-0/50006-3).

Eisenberg JF & Rerdford KH 1999 In *Mammals of the Neotropics: the Central Neotropics, Ecuador, Peru, Bolivia, Brazil*, 3rd edn, p 609. Chicago: University of Chicago Press.

Fawcett DW, Eddy EM & Phillips DM 1970 Observations on the fine structure and relationships of the chromatoid body in mammalian spermatogenesis. *Biology of Reproduction* **2** 129–153. (doi:10.1095/biolreprod2.1.129)

França LR & Russell LD 1998 The testis of domestic animals. In *Male Reproduction: a Multidisciplinary Overview*, 1st edn, pp 197–219. Eds J Regadera & F Martinez-Garcia. Madrid: Churchill Livingstone.

França LR, Silva VA Jr, Chiarini-Garcia H, Garcia SK & Debeljuk L 2000 Cell proliferation and hormonal changes during postnatal development of the testis in the pig. *Biology of Reproduction* **63** 1629–1636. (doi:10.1095/biolreprod63.6.1629)

Góes RM & Dolder H 2002 Cytological steps during spermiogenesis in the house sparrow (*Passer domesticus* Linnaeus). *Tissue & Cell* **34** 273–282. (doi:10.1016/S0040-8166(02)00017-4)

Gunawardana VK & Scott MG 1977 Ultrastructural studies on the differentiation of spermatids in the domestic fowl. *Journal of Anatomy* **124** 741–755.

Hoffer AP 1982 Ultrastructural studies of the seminiferous and epididymal epithelium and epididymal sperm in rats treated with gossypol. *Contraceptive Delivery Systems* **3** 278.

IUCN 2013 IUCN Red List of Threatened Species, version 2013.1 (www.iucnredlist.org, downloaded on 03 September 2013).

Lalli M & Clermont Y 1981 Structural changes of the head components on the rat spermatid during late spermiogenesis. *American Journal of Anatomy* **160** 419–434. (doi:10.1002/aja.1001600406)

Lin M & Jones RC 1993 Spermiogenesis and spermiation in Japanese quail (*Coturnix coturnix japanonica*). *Journal of Anatomy* **183** 525–535.

Maekawa M, Kamimura K & Nagano T 1996 Peritubular myoid cells in the testis: their structure and function. *Archives of Histology and Cytology* **59** 1–13. (doi:10.1679/aohc.59.1)

Oliveira MF, Mess A, Ambrósio CE, Dantas AG, Favaron PO & Miglino MA 2008 Chorioallantoic placentation in *Galea spixii* (Rodentia, Caviomorpha, Caviidae). *Reproductive Biology and Endocrinology* **6** 39. (doi:10.1186/1477-7827-6-39)

Pesch S & Bergmann M 2006 Structure of mammalian spermatozoa in respect to viability and cryopreservation. *Micron* **37** 597–612. (doi:10.1016/j.micron.2006.02.006)

Renfree M, Wilson J, Short R, Shaw G & George F 1992 Steroid hormone content of the gonads of the Tammar Wallaby during sexual differentiation. *Biology of Reproduction* **47** 644–647. (doi:10.1095/biolreprod47.4.644)

Russell LD 1993 Morphological and functional evidence for Sertoli-germ cells relationships. In *The Sertoli Cell*. (LD Russell and MD Griswold, eds) pp 39–86. Clearwater, Florida: Cache River Press.

Russell LD, Ren HP, Sinha-Hikim I, Schulze W & Sinha-Hikim AP 1990 A comparative study in twelve mammalian species of volume densities, volumes and numerical densities of selected testis components, emphasizing those related to the Sertoli cell. *American Journal of Anatomy* **188** 21–30. (doi:10.1002/aja.1001880104)

Santos PRS, Carrara TVB, Silva LCS, Silva AR, Oliveira MF & Assis Neto AC 2011 Caracterização morfológica e frequência dos estádios do ciclo do epitélio seminífero em preás (*Galea spixii* Wagler, 1831) criados em cativeiro. *Pesquisa Veterinária Brasileira* **31** 18–24. (doi:10.1590/S0100-736X2011001300004)

Santos PRS, Oliveira MF, Silva AR & Assis Neto AC 2012*a* Development of spermatogenesis in captive-bred Spix's yellow-toothed cavy (*Galea spixii*). *Reproduction, Fertility, and Development* **24** 877–885. (doi:10.1071/RD12015)

Santos PRS, Oliveira MF, Silva AR, Camargo CM & Assis Neto AC 2012*b* The microstructure and development of male genital organs of Spix's yellow-toothed cavy (*Galea spixii*) bred in captivity. *Pesquisa Veterinária Brasileira* **32** 84–90. (doi:10.1590/S0100-736X2012001300015)

Schleirmacher E & Schmidt W 1973 Changes of the synaptonemal complex at the end of pachytene. *Humangenetik* **19** 235–245. (doi:10.1007/BF00295237)

Segatelli TM, Almeida CCD, Pinheiro PFF, Martinez M, Padovani CR & Martinez FE 2002 Kinetics of spermatogenesis in the Mongolian gerbil (*Meriones unguiculatus*). *Tissue & Cell* **34** 7–13. (doi:10.1054/tice.2002.0218)

Singwi MS & Lall SB 1983 Spermatogenesis in the non-scrotal bat – *Rhinopoma kinneari* Wroughton (Microchiroptera: Mammalia). *Acta Anatomica* **116** 136–145. (doi:10.1159/000145735)

Skinner MK 2005 Sertoli cell–somatic cell interactions. In *Sertoli Cell Biology*, pp 317–328. Eds MK Skinner & MD Griswold. San Diego: Elsevier Academic Press.

Smithwick EB, Young LG & Gould KG 1996 Duration of spermatogenesis and relative frequency of each stage in the seminiferous epithelial cycle of the chimpanzee. *Tissue & Cell* **28** 357–366. (doi:10.1016/S0040-8166(96)80022-X)

Solari AJ & Moses MJ 1973 The structure of the central region in the synaptonemal complexes hamster and cricket spermatocytes. *Journal of Cell Biology* **56** 145–152. (doi:10.1083/jcb.56.1.145)

Sud B 1961 Morphological and histochemical studies of the chromatoid body and related elements in spermatogenesis of the rat. *Quarterly Journal of Microscopical Science* **102** 495–505.

Von Ubisch G & Amaral JP 1935 Diferença de capacidade de imunização da cobaia (*Cavia porcellus*, L) e do preá (*Cavia rufescens*, Lund) contra a anatoxina diftérica. *Memórias do Instituto Butantan* **10** 179–189.

Warburg O 1966 Oxygen, the creator of differentiation. In *Current Aspects of Biochemical Energetics*, pp 103–109. Eds NO Kaplan & E Kennedy. London–New York: Academic Press.

Watanabe I & Yamada E 1983 The fine structure of lamellated nerve endings found in the rat gingiva. *Archivum Histologicum Japonicum. Nippon Soshikigaku Kiroku* **46** 173–182.

Wildt DE 2005 Lions, tigers, and pandas, oh my. *Journal of Andrology* **26** 452–454. (doi:10.2164/jandrol.05046)

Williamson P, Fletcher TP & Renfree MB 1990 Testicular development and maturation of the hypothalamic–pituitary–testicular axis in the male tammar, *Macropus eugenii*. *Journal of Reproduction and Fertility* **88** 549–557. (doi:10.1530/jrf.0.0880549)

Zirkin B, Ewing L, Kromann N & Cochran R 1980 Testosterone secretion by rat, rabbit, guinea pig, dog, and hamster testes perfused *in vitro*: correlation with Leydig cell ultrastructure. *Endocrinology* **107** 1867–1874. (doi:10.1210/endo-107-6-1867)

Received 15 September 2013
First decision 7 October 2013
Accepted 7 October 2013